Cranial asymmetry in Eocene archaeocete whales and the evolution of directional hearing in water

Julia M. Fahlke[a,1], Philip D. Gingerich[a,b], Robert C. Welsh[c], and Aaron R. Wood[a,d]

[a]Museum of Paleontology, [b]Department of Geological Sciences, and [c]Department of Radiology, University of Michigan, Ann Arbor, MI 48109; and [d]Department of Geology and Geological Engineering, Paleontology Research Laboratory, South Dakota School of Mines and Technology, Rapid City, SD 57701

Edited by David B. Wake, University of California, Berkeley, CA, and approved July 28, 2011 (received for review June 2, 2011)

Eocene archaeocete whales gave rise to all modern toothed and baleen whales (Odontoceti and Mysticeti) during or near the Eocene-Oligocene transition. Odontocetes have asymmetrical skulls, with asymmetry linked to high-frequency sound production and echolocation. Mysticetes are generally assumed to have symmetrical skulls and lack high-frequency hearing. Here we show that protocetid and basilosaurid archaeocete skulls are distinctly and directionally asymmetrical. Archaeocete asymmetry involves curvature and axial torsion of the cranium, but no telescoping. Cranial asymmetry evolved in Eocene archaeocetes as part of a complex of traits linked to directional hearing (such as pan-bone thinning of the lower jaws, mandibular fat pads, and isolation of the ear region), probably enabling them to hear the higher sonic frequencies of sound-producing fish on which they preyed. Ultrasonic echolocation evolved in Oligocene odontocetes, enabling them to find silent prey. Asymmetry and much of the sonic-frequency range of directional hearing were lost in Oligocene mysticetes during the shift to low-frequency hearing and bulk-straining predation.

Cetacea | land-to-sea transition

Most mammals have bilaterally symmetrical skulls. Symmetrical crania characterize the artiodactyls closely related to whales, and symmetrical crania characterize mysticetes within Cetacea (1) (Fig. 1*A*). Odontocetes are exceptional because most odontocete crania are asymmetrical, with dorsal cranial bones shifted posteriorly and to the left side (1–8). Living odontocetes have a hypertrophied melon, nasal sacs, and phonic lips used to produce high-frequency sound (> 20 kHz) (9–11). Mysticetes lack these specializations of the nasal apparatus, use low-frequency sound (11, 12), and may use the larynx (13) to produce low-frequency sound. Coupling of high-frequency echolocation with facial and cranial asymmetry in living odontocetes, and the absence of both in living artiodactyls and living mysticetes, make it reasonable to expect that asymmetry originated in odontocetes (5–7). However, it is unresolved how the cranial asymmetry of odontocetes evolved in the transition from archaeocetes to modern whales, and the history becomes even more complex when archaeocetes themselves are considered.

Eocene archaeocete whales gave rise to all modern toothed and baleen whales during or near the Eocene-Oligocene transition (14–16). Archaeocetes were previously thought to have symmetrical skulls (3, 5, 7). Asymmetry observed in fossil crania has often been assumed to be an artifact of deformation following burial, and it has been ignored or even removed in published drawings [as was done initially for three of the skulls we studied (17–19)].

Results

Here we document and quantify asymmetry in archaeocete crania. Further observations on exceptionally well-preserved archaeocete crania and dentaries suggest a link between cranial asymmetry and the ability to locate sound sources in water.

We quantified midline suture deviation, δx, from a straight rostrocaudal axis [RC, after Ness (4)] for undeformed crania of two protocetid (*Artiocetus clavis* and *Qaisracetus arifi*) and four basilosaurid archaeocetes (two *Basilosaurus isis* and two *Dorudon atrox*) (Fig. S1).

The oldest archaeocete in our study that shows cranial asymmetry is *A. clavis*, a protocetid from the early middle Eocene (47 Ma) of Pakistan (18) (Fig. 1). The holotype skull (GSP-UM 3458) (Fig. 1*B*) was found palate-up in marl with no evident compression or deformation (18), and yet the dorsal midline suture deviates notably from RC.

Archaeocete asymmetry, like that of odontocetes (4), is variable in amount but consistent in direction. To quantify the asymmetry we calculated mean relative deviations (mean δx/RC) of undeformed archaeocete crania and compared these to a model distribution based on measurements of 24 symmetrical artiodactyls (Fig. 2). The model distribution is normally distributed with a mean of zero and with the empirical variance estimated from the artiodactyl sample (standard deviation $s = 0.0045$ mm/mm) (yellow reference bands in Fig. 2). All six archaeocete skulls studied here have mean deviations that are positive in sign, indicating consistent and significant midcranial deviation to the right of RC. The six archaeocete crania, taken together, have midline suture deviations significantly greater in amount than expected for symmetrical skulls. Four of the six archaeocetes, considered individually, have midline suture deviations significantly greater than expected (for statistics, see Tables S1 and S2).

The probability of having all six archaeocete crania right-deviated if sampled from a symmetrical population is $(0.5)^6 = 0.016$. This probability is substantially less than 0.05, and the archaeocete sample in Fig. 2 is significantly directional. The dorsal midline suture is a curved rather than straight line (Fig. S1), and a midline suture lying to the right of RC means that the studied crania bend to the left. This curvature is similar to that seen in odontocetes. However, the posterior-leftward shift of cranial bones near the cranial vertex associated with telescoping (2) has moved the odontocete midline suture to the left of RC near the back of the skull (4).

In archaeocetes, the midline suture seems to deviate most strongly from RC along the nasal, frontal, and parietal bones, when viewed dorsally. However, Heyning (7) stated that shapes of paired left and right cranial bones of odontocetes can differ substantially without greatly influencing the dorsal midline of a skull. If true, then the full extent of cranial asymmetry cannot be captured by study of the midline suture in the dorsal view alone. To test this idea we developed a more general measure of asymmetry that compares dorsal and ventral midline sutures of the cranium simultaneously. This measure was applied to a digital surface

Author contributions: J.M.F., P.D.G., and A.R.W. designed research; J.M.F., P.D.G., and R.C.W. performed research; A.R.W. contributed new analytic tools; J.M.F., P.D.G., R.C.W., and A.R.W. analyzed data; and J.M.F. and P.D.G. wrote the paper.

The authors declare no conflict of interest.

This article is a PNAS Direct Submission.

Freely available online through the PNAS open access option.

[1]To whom correspondence should be addressed. E-mail: jfahlke@umich.edu.

This article contains supporting information online at www.pnas.org/lookup/suppl/doi:10.1073/pnas.1108927108/-/DCSupplemental.

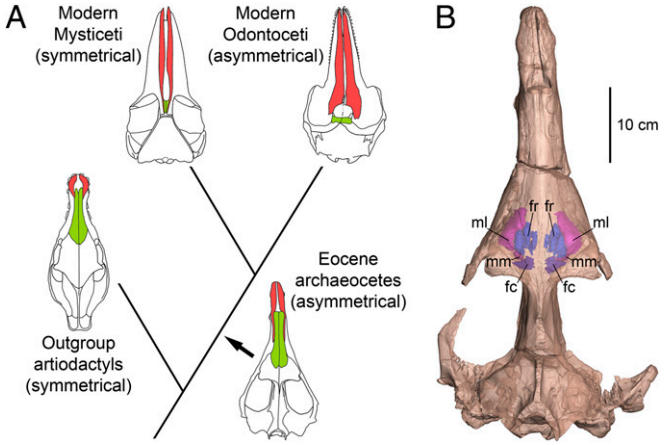

Fig. 1. Asymmetry in the evolution of whales. (*A*) Evolutionary relationships between terrestrial Artiodactyla, Eocene archaeocetes, and modern Mysticeti and Odontoceti. Cranial asymmetry is present in archaeocetes and Odontoceti, but absent in artiodactyls and Mysticeti. Archaeocetes are represented by *Artiocetus*, Mysticeti are represented by *Balaenoptera*, Odontoceti are represented by *Tursiops*, and terrestrial artiodactyls are represented by *Elomeryx*. (*B*) Skull of the protocetid archaeocete *A. clavis* (GSP-UM 3458) in dorsal view showing maxillary and frontal sinuses visible in a 3D micro-CT reconstruction. Note the rightward deviation of the mid-cranium. fc, caudal frontal sinus; fr, rostral frontal sinus; ml, lateral maxillary sinus; mm, medial maxillary sinus.

model of the cranium of *A. clavis* computed from CT scans. The red line in Fig. 3 represents successive deflection angles of the dorsal and ventral midline sutures from the vertical sagittal midplane in consecutive transverse sections. This representation shows that cranial asymmetry in *Artiocetus* involves 3D torsion about an anteroposterior axis, affecting the whole cranium. Viewed from the braincase forward, the torsion is clockwise and increases anteriorly, being greatest in the rostrum. Rightward deviation of the dorsal midline suture reflects intersection of the

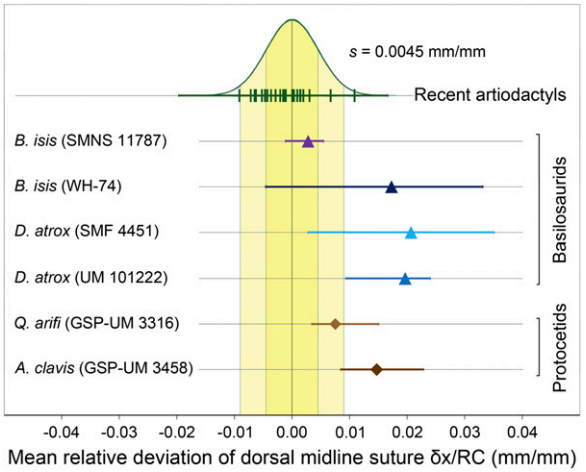

Fig. 2. Mean relative deviation of the dorsal midline suture from RC (mean δx/RC) for archaeocete crania. Means are calculated for lateral deviations (mm) at nine evenly spaced points along RC (mm) for each specimen. Mean δx/RC for 24 artiodactyl specimens (included taxa are given in Table S1) serve as modern symmetrical comparison and show a normal distribution with zero mean and standard deviation s = 0.0045 (green curve; one and two standard deviation intervals highlighted in yellow). Note that archaeocete midline sutures deviate consistently to the right, and that the deviation is statistically significant in four of six cases.

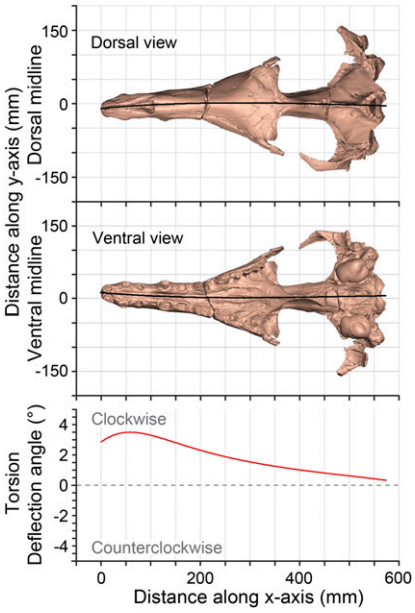

Fig. 3. Torsion of the cranium of the middle Eocene protocetid *Artiocetus clavis* (GSP-UM 3458). Absolute deviations of dorsal and ventral midline sutures (black lines) are shown in dorsal and ventral view, respectively. Torsion is documented by successive deflection angles, where each is the angle between a line connecting dorsal and ventral midline points, measured from the *xz*-plane, for 1,000 successive values of *x*. Note that torsion is clockwise and greatest in the rostrum.

cranial surface with an axially torted midline plane, and "axial torsion" is a more inclusive descriptor of the asymmetry involved. Axial torsion has not yet been quantified in odontocetes.

Dentaries of protocetid and basilosaurid archaeocetes have large odontocete-like mandibular foramina on their lingual surfaces and large mandibular canals (20, 21). Furthermore, exceptionally preserved dentaries of *B. isis* (WH-74) (Fig. 4) show distinct thinning of the outer wall of the dentary indicative of the "pan bone" found in modern Odontoceti (22). The large mandibular canals in protocetids and basilosaurids indicate the presence of a mandibular fat body similar to that of modern odontocetes. The fat body of odontocetes has an acoustic impedance close to that of seawater (22) and functions as a wave guide, conducting underwater sound received via vibration of the pan bone and through the mandibular foramen to the auditory bulla (10, 22–24).

The pan bone in *B. isis* is located in front of the mandibular foramen and not, as in odontocetes (22), directly opposite it. The position of the pan bone in *B. isis* is asymmetrical, with the thinnest area being about 9 cm more rostral and 5 cm more ventral on the left side (Fig. 4). This finding is surprising because the positions of mandibular foramina on the lingual sides of the left and right dentaries appear symmetrical. It is not yet known whether the pan bone is asymmetrical in other archaeocete specimens. Pan bone thicknesses for archaeocetes in the literature are questionable because they were measured through the mandibular foramen (25), but our CT imagery of dentary wall thickness shows the pan-bone thinning of archaeocetes to be farther forward (Fig. 4).

Discussion

Recognition of directional cranial asymmetry in archaeocetes has a number of implications for our understanding of the evolution of hearing in whales. Heyning (7) hypothesized that directional asymmetry in odontocetes evolved to minimize interference cancellation of sound produced in parallel narial passages, and it is common to assume that odontocete asymmetry is related to sound production and biosonar (4, 5, 7, 22). However, *A. clavis* retained

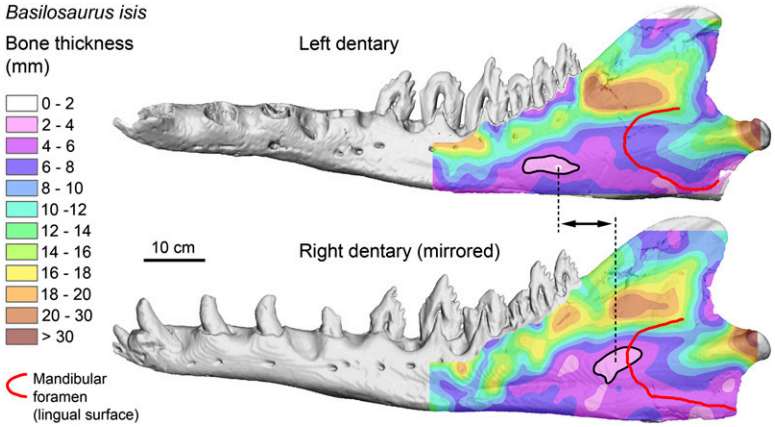

Fig. 4. Bone thickness of the lateral wall of the left and right (mirrored) dentaries of late Eocene *B. isis* (WH-74). Note that the thinnest area (pan bone, outlined in black) lies in front of the mandibular foramen (red line) in each dentary. Note also the asymmetrical positions of the pan bones.

an extensive system of air sinuses that inflated the cranial bones (maxillary and frontal sinuses are shown in Fig. 1*B*). Frontal sinuses are also known from middle Eocene Remingtonocetidae (26) and late Eocene Basilosauridae (17, 19, 27). Large endoturbinates, which are not seen in odontocetes (28), are present in *A. clavis*. Modification of nasal pathways that would enable biosonar started after cranial torsion was well developed and thus cannot be the cause of asymmetry.

MacLeod et al. (29) hypothesized that asymmetry evolved to enable swallowing large, whole prey. However, archaeocetes retained shearing teeth and chewed their food before swallowing. Reduction of tooth size and loss of shearing occlusion started after asymmetry was well developed, and so swallowing whole prey cannot be the cause of asymmetry.

Development of archaeocete skull asymmetry coincides with the appearance of enlarged mandibular foramina, pan bones, fat-pad wave guides (as shown above), and development of enlarged tympanic bullae and pterygoid sinuses (30). Consequently, we conclude that directional asymmetry in archaeocetes is related to hearing. This finding is consistent with odontocete ontogeny: at perinatal stages, spotted dolphins (*Stenella attenuata*) exhibit incipient cranial and facial asymmetry, whereas the mandibular fat body and pan bone are already fully developed (31). Cranial asymmetry reaches an adult degree soon after birth in the harbor porpoise *Phocoena phocoena* (6).

Directional asymmetry enhances the ability of owls to locate prey in the dark by decomposing complex sound (32), and we envision a similar enhancement of hearing in archaeocetes. Thus, the position-dependent spectral filtering used to localize sound in odontocetes (33) probably evolved first in archaeocetes. The range of frequencies involved is still an open question.

Asymmetry in archaeocetes is most likely part of a complex of anatomical characteristics enhancing predation by using sound. However, archaeocetes lack osteological evidence of the specialized organs required to produce high-frequency sound (melon, nasal sacs, phonic lips) (9, 10). The sounds they heard likely came from prey that produced sounds at frequencies that archaeocetes could detect and process. Fish sound is normally in the midsonic range (1–4 kHz), but fish also produce stridulation sounds up to 10 kHz, and schooling pelagic fish produce intense complex sound with high-frequency components (34). Sound in the 4- to 10-kHz range, near the lower limit for sound produced by odontocetes, has corresponding wavelengths in seawater of 40 to 10 cm. These are probably the ranges of frequencies and wavelengths involved in hearing in archaeocetes like *A. clavis*.

We propose the following sequence and timing for the evolution of cranial asymmetry in whales: (*i*) Middle to late Eocene protocetid and basilosaurid archaeocetes: initial torsion evolved in concert with the development of directional hearing of high sonic-frequency sound in water, thinning of pan bones, and development of mandibular wave guides; (*ii*) Oligocene and later Odontoceti: high-frequency sound production and active echolocation evolved, linked to modification of nasal structures and a leftward and posterior shift of cranial bones, soon after the divergence from Mysticeti; and (*iii*) Oligocene and later Mysticeti: cranial asymmetry was reduced along with loss of the pan bones and mandibular wave guides when mysticetes shifted to low-frequency hearing and bulk-straining predation. Transitions between each of these stages can be documented in the fossil record and deserve careful study.

Methods

Asymmetry of bones is referred to as "cranial asymmetry," whereas soft tissue asymmetry is referred to as "facial asymmetry" (7). Cranial asymmetry can be quantified by measuring the deviation of the dorsal midline suture, δx, from RC (4). We divided RC into 10 segments and measured the corresponding nine deviations for two protocetid (*A. clavis* and *Q. arifi*) and four basilosaurid (two *B. isis* and two *D. atrox*) crania. We only used crania of adult individuals that showed no taphonomical deformation. Twenty-four modern artiodactyl crania were measured as a symmetrical comparative sample. The mean relative deviation (mean δx/RC) for each sample was calculated and compared.

We CT-scanned the cranium of *A. clavis* (GSP-UM 3458) and the dentaries of *B. isis* (WH-74) in the Department of Radiology at the University of Michigan and generated 3D surface models. These models were then oriented in a global *x-y-z* coordinate system. Torsion of the cranium of *A. clavis* was measured by calculating the deflection angle (i.e., the angle of deviation of a line connecting dorsal and ventral midline sutures from the *xz*-plane at 1,000 points along the *x* axis of the cranium). Frontal and maxillary sinuses of *A. clavis* were reconstructed from micro-CT scans made at the Steinmann-Institut, University of Bonn. Bone thickness of the outer walls of both dentaries of *B. isis* was measured from CT scans. For detailed description of materials and methods, see *SI Methods*.

ACKNOWLEDGMENTS. We thank W. Sanders and J. Klausmeyer for fossil preparation and reconstruction; H. DeMarsh, M. Muck, I. Ruf, P. Göddertz, and G. Oleschinski for CT scanning and images; P. Missiaen for help with photography; S. Heise and S. O'Grady for access to and help with Materialise software; E. P. J. Heizmann, R. Brocke, G. Gunnell, P. Tucker, and S. Hinshaw for access to collections; and D. C. Fisher for reading the manuscript. Research was supported by a Feodor Lynen Fellowship (Alexander von Humboldt Foundation), National Geographic Society Grant 7726-04, and National Science Foundation Grants EAR-0517773 and 0920972.

1. Feldhamer GA (2007) *Mammalogy: Adaptation, Diversity, Ecology* (Johns Hopkins University Press, Baltimore), p 643.
2. Miller GS (1923) The telescoping of the cetacean skull. *Smithsonian Miscellaneous Collections* 76:1–70.
3. Slijper EJ (1936) Die Cetaceen, Vergleichend-Anatomisch und Systematisch (Cetacea, comparative anatomy and systematics). *Capita Zoologica*, 6–7:1–590 (in German).
4. Ness AR (1967) A measure of asymmetry of the skulls of odontocete whales. *J Zool* 153:209–211.
5. Mead JG (1975) Anatomy of the external nasal passages and facial complex in the Delphinidae (Mammalia: Cetacea). *Smithson Contrib Zool* 207:1–72.
6. Yurick DB, Gaskin DE (1988) Asymmetry in the skull of the harbour porpoise *Phocoena phocoena* (L.) and its relationship to sound production and echolocation. *Can J Zool* 66:399–402.
7. Heyning JE (1989) Comparative facial anatomy of beaked whales (Ziphiidae) and a systematic revision among the families of extant Odontoceti. *Natural History Museum of Los Angeles County Contributions in Science* 405:1–64.
8. Berta A, Sumich JL, Kovacs KM (2006) *Marine Mammals: Evolutionary Biology* (Elsevier, Amsterdam), 2nd Ed, p 547.
9. Cranford TW, Amundin M, Norris KS (1996) Functional morphology and homology in the odontocete nasal complex: Implications for sound generation. *J Morphol* 228: 223–285.
10. Cranford TW, Krysl P, Hildebrand JA (2008) Acoustic pathways revealed: Simulated sound transmission and reception in Cuvier's beaked whale (*Ziphius cavirostris*). *Bioinspir Biomim* 3:016001.
11. Ketten DR (1997) Structure and function in whale ears. *Bioacoustics* 8:103–136.
12. Ketten DR (1992) The marine mammal ear: Specializations for aquatic audition and echolocation. *The Evolutionary Biology of Hearing*, eds Webster DB, Fay RR, Popper AN (Springer-Verlag, New York), pp 717–750.
13. Reidenberg JS, Laitman JT (2007) Discovery of a low frequency sound source in Mysticeti (baleen whales): Anatomical establishment of a vocal fold homolog. *Anat Rec (Hoboken)* 290:745–759.
14. Fordyce RE, Barnes LG (1994) The evolutionary history of whales and dolphins. *Annu Rev Earth Planet Sci* 22:419–455.
15. Fordyce RE, de Muizon C (2001) Evolutionary history of cetaceans: A review. *Secondary Adaptations of Tetrapods to Life in Water*, eds Mazin J-M, de Buffrénil V (Verlag Friedrich Pfeil, Munich), pp 169–233.
16. Gingerich PD (2005) Cetacea. *Placental Mammals: Origin, Timing, and Relationships of the Major Extant Clades*, eds Rose KD, Archibald JD (Johns Hopkins University Press, Baltimore), pp 234–252.
17. Stromer E (1908) Die Archaeoceti des ägyptischen Eozäns (Archaeocetes of the Egyptian Eocene). *Beiträge zur Paläontologie und Geologie Österreich-Ungarns und des Orients, Vienna*, 21:106–178 (in German).
18. Gingerich PD, Haq MU, Zalmout IS, Khan IH, Malkani MS (2001) Origin of whales from early artiodactyls: Hands and feet of Eocene Protocetidae from Pakistan. *Science* 293: 2239–2242.
19. Uhen MD (2004) Form, function, and anatomy of *Dorudon atrox* (Mammalia, Cetacea): An archaeocete from the middle to late Eocene of Egypt. *University of Michigan Papers on Paleontology* 34:1–222.
20. Müller J (1849) *Über die fossilen Reste der Zeuglodonten von Nordamerika, mit Rücksicht auf die europäischen Reste aus dieser Familie* (*On Fossil Zeuglodonts of North America with Reference to European Remains of this Family*) (G. Reimer Verlag, Berlin) pp 1–38 (in German).
21. Bajpai S, Gingerich PD (1998) A new Eocene archaeocete (Mammalia, Cetacea) from India and the time of origin of whales. *Proc Natl Acad Sci USA* 95:15464–15468.
22. Norris KS (1968) The evolution of acoustic mechanisms in odontocete cetaceans. *Evolution and Environment*, ed Drake ET (Yale University Press, New Haven), pp 297–324.
23. Cranford TW, Krysl P, Amundin M (2010) A new acoustic portal into the odontocete ear and vibrational analysis of the tympanoperiotic complex. *PLoS ONE* 5:e11927.
24. Montie EW, Manire CA, Mann DA (2011) Live CT imaging of sound reception anatomy and hearing measurements in the pygmy killer whale, *Feresa attenuata*. *J Exp Biol* 214:945–955.
25. Nummela S, Thewissen JGM, Bajpai S, Hussain T, Kumar K (2007) Sound transmission in archaic and modern whales: Anatomical adaptations for underwater hearing. *Anat Rec (Hoboken)* 290:716–733.
26. Bajpai S, Thewissen JGM, Conley RW (2011) Cranial anatomy of middle Eocene *Remingtonocetus* (Cetacea, Mammalia) from Kutch, India. *J Paleontol* 85:703–718.
27. Kellogg R (1936) A review of the Archaeoceti. *Carnegie Institution of Washington Publications* 482:1–366.
28. Mead JG, Fordyce RE (2009) The therian skull—A lexicon with emphasis on the odontocetes. *Smithson Contrib Zool* 627:1–248.
29. MacLeod CD, et al. (2007) Breaking symmetry: The marine environment, prey size, and the evolution of asymmetry in cetacean skulls. *Anat Rec (Hoboken)* 290:539–545.
30. Luo Z, Gingerich PD (1999) Terrestrial Mesonychia to aquatic Cetacea: Transformation of the basicranium and evolution of hearing in whales. *University of Michigan Papers on Paleontology* 31:1–98.
31. Rauschmann MA, Huggenberger S, Kossatz LS, Oelschläger HHA (2006) Head morphology in perinatal dolphins: A window into phylogeny and ontogeny. *J Morphol* 267:1295–1315.
32. Norberg RA (1978) Skull asymmetry, ear structure and function, and auditory localization in Tengmalm's Owl, *Aegolius funereus* (Linne). *Philos Trans R Soc Lond B Biol Sci* 282:325–410.
33. Branstetter BK, Mercado E (2006) Sound localization by cetaceans. *Int J Comp Psychol* 19:26–61.
34. Kasumyan AO (2008) Sounds and sound production in fishes. *J Ichthyol* 48:981–1030.